Recent Results from CDF

Michele Gallinaro
The Rockefeller University
1230 York Ave., New York, NY 10021, USA
michgall@fnal.gov

Abstract

We present the latest results from the CDF experiment at the Tevatron Collider in $p\bar{p}$ collisions at $\sqrt{s}$ = 1.8 TeV. The large data sample collected during Run 1, from 1992 until 1995, allows measurements in many domains of high–energy physics. Here, we report on the first measurement of $\sin(2\beta)$, a CP violation parameter, and on an improved measurement of the top quark cross section. We also report on searches for the so–far elusive Higgs boson, and for SUSY, through searches for direct production of top and bottom scalar quarks. Finally, we outline the prospects for the physics during the upcoming Run 2, ready to start in the upcoming year 2000.

1 Introduction

At the Tevatron Collider bunches of protons and antiprotons are accelerated and collided at an energy of $\sqrt{s} = 1.8$ TeV. The Collider Detector at Fermilab (CDF) and DØ detectors have collected large samples of data. Here, we present some of the latest results from the CDF experiment. Data were collected during two periods: Run 1A groups about 20 pb^{-1} and Run 1B about 90 pb^{-1}, for a total period of time that goes from 1992 until the end of 1995.

The CDF detector [1] relies on a high resolution tracking system with a central tracking drift chamber immersed in a 1.4 Tesla magnetic field. In addition, a high precision silicon micro-vertex detector was added inside the drift chamber and near the beam–pipe to allow for precise vertex determination. Outside the tracking system, electromagnetic and hadronic calorimeters provide excellent measurement of particle energy. Muon chambers located outside the magnetic yoke complete the tracking system.

The results presented here include the direct measurement of the CP violation parameter of $\sin(2\beta)$. Recently, the CDF collaboration also improved the measurement of the $t\bar{t}$ production cross section, and continues the investigation for new physics, including Higgs boson and SUSY searches. We conclude the paper and highlight the improved capabilities in Run II, and summarize the upgrade projects under construction for the CDF detector.

2 CP Violation: measurement of $\sin(2\beta)$

The origin of CP violation has been an outstanding problem since its first discovery in $K^0_L \rightarrow \pi^+\pi^-$ decays. After 35 years of the discovery of CP violation, the kaon system was still the only place where CP violation had been observed. However, neutral B mesons are expected to yield large CP violating effects. Here, we report on a direct measurement that indicates a CP violation effect in $B^0 \rightarrow J/\Psi K^0_s$ decays.

CP violation can be explained in an elegant way in the Standard Model (SM) with three generations, as suggested by Cabibbo, Kobayashi and Maskawa [2]. They proposed that quark mixing is the cause. The CKM matrix relates the mass and weak eigenstates of the quarks. With three generations of quarks, the CKM matrix has a physical complex phase capable of accommodating CP violation.

Similar to the kaon system, CP violating effects are expected in B mesons. The effects of CP violation in the inclusive decay channels of the B mesons are still too small ($\sim 10^{-3}$) to be detected [3]. Yet, the interference due to mixing of B_d^0 decays to the same CP state could show large violations. CP violation can manifest itself as an asymmetry in the decay rate of particle versus anti-particle to a particular CP eigenstate. For example, a B_d^0 may decay directly to $J/\Psi K_s^0$, or it may oscillate to a $\overline{B_d^0}$ and then decay to $J/\Psi K_s^0$. The two paths have a phase difference and the interference results in an asymmetry:

$$\mathcal{A}_{CP}(t) = \frac{\overline{B_d^0}(t) - B_d^0(t)}{\overline{B_d^0}(t) + B_d^0(t)} = sin(2\beta) \cdot sin(\Delta m_d t),$$

where $B_d^0(t)$ $[\overline{B_d^0}(t)]$ is the number of $J/\Psi K_s^0$ decays at proper time t from mesons produced as B_d^0 $[\overline{B_d^0}]$, and $sin(\Delta m_d t)$ is the mixing oscillation due to the decay interference. In the SM, the CP asymmetry is proportional to $\sin 2\beta$, where β is an angle of the unitarity triangle. In order to measure the asymmetry $\mathcal{A}_{CP}$ we have to identify the flavor of the B meson at the time of production. Unfortunately, the tagging algorithms are not perfect, and the "true" asymmetry is "diluted" by a dilution factor (D) that takes into account the "mistakes" of the tagging algorithms, which incorrectly identify the flavor. The dilution factor is defined as $D = 2P - 1$, where P is the probability to have a correct tag. Therefore, the observed asymmetry $\mathcal{A}_{CP}^{obs} = D \cdot \mathcal{A}_{CP}$, is reduced by the dilution parameter.

We take advantage of the large B meson production cross section at the Tevatron, and use a sample of $J/\Psi K_s^0$ decays to measure $\sin 2\beta$. This measurement uses a data sample which is larger by a factor of two with respect to our previous measurement [4] by including $J/\Psi K_s^0$ events not reconstructed in the SVX. Here, in addition to the tagging algorithm which we previously used in Ref. [4], we also employ two additional tagging algorithms which further enlarge the effective statistical power our sample size. We reconstruct $B \to J/\Psi K_s^0$ events similarly to previous analyses at CDF. Then, we categorize the events according to the tagging algorithm used. We measure dilutions and efficiencies for each class of events and use a maximum likelihood fitting procedure to extract the result for $\sin 2\beta$.

We reconstruct J/Ψ events decaying to $\mu^+\mu^-$. We identify K_s^0 candidates by reconstructing oppositely charged tracks to the $K_s^0 \to \pi^+\pi^-$ hypothesis. We constrain the $\mu^+\mu^-$ and $\pi^+\pi^-$ pairs to the world average masses. The reconstructed invariant mass of the $\mu^+\mu^-\pi^+\pi^-$ system for all the candidates is shown in Figure 1. About one half (202±18 events as opposed to 193±26 events) of the final B° signal sample contains a precise lifetime information as both muons are contained in the silicon vertex detector (SVX). The precise lifetime information allows us to make a time–dependent measurement of the oscillation. We can also use the events that are not contained within the SVX acceptance. In this case, CP asymmetry is still present in the form of a time–integrated measurement. The statistical power is only reduced by a factor of one third in our non–SVX sample, where the lifetime information is lost.

The measurement of $\mathcal{A}_{\mathcal{CP}}$ is possible if we can determine the flavor (B or $\overline{B}$) of the B meson at the time of production. A tagging method with dilution D and tagging efficiency ϵ yields an uncertainty on $\sin 2\beta$ which scales as $1/\sqrt{\epsilon D^2 N}$, with N events. Therefore, ϵD^2 measures the effective tagging power. Here, we use a combination of different tagging methods. We use three taggers. We use a Same Side Tagger (SST), which relies on selecting a track (supposedly from a $\pi^\pm$) near the B meson, and it is correlated to the b–flavor [5]. The SST tag is a candidate track with a $p_T > 400$ MeV/c, reconstructed in the SVX. The SST tagger was used in our earlier measurement of $\sin 2\beta$. The SST dilution is measured to be $(16.6 \pm 2.2)\%$ in the $J/\Psi K_s^0$ sample, for events reconstructed in the SVX. Here, we extend the SST algorithm to events outside the SVX coverage (we drop the impact parameter cut), and we find a dilution factor of $(17.4 \pm 3.6)\%$.

In order to further increase the effective number of candidate events, we use two additional taggers that determine the flavor of the "other" B meson; we can also refer to them as "opposite side taggers". We use the Soft Lepton Tagger (SLT) which determines the charge of the lepton from the $b \to l$ decay [6]. Lepton tracks have a $p_T > 1(2)$ GeV/c^2 for electrons (muons). The dilution is measured from $B^+ \to J/\Psi K^+$ sample and we find $D = 62.5 \pm 14.6\%$. The other opposite side tagger is a Jet Charge (JETQ) tagger [7]. The flavor is determined by a measure of the average of the charge of the opposite side jet. The jet is formed by an algorithm that combines tracks ($p_T > 0.4$ GeV/c) around a seed track with $p_T > 1.75$ GeV/c, up to the mass of the B. The dilution again is measured from $B^+ \to J/\Psi K^+$ sample, and is $23.5 \pm 6.9\%$.

In general, the ideal tagger should have high dilution and high efficiency. In reality, the SLT tagger has high dilution but low efficiency, while both SST and JETQ taggers have higher efficiency and low dilution values. By coincidence, all of the three taggers measured $\epsilon D^2 \sim 2\%$. Therefore, we have effectively tripled the size of our event sample with respect to [4]. The combined ϵD^2 for the three taggers is $6.3 \pm 1.7\%$. In conclusion, our sample of 400 events corresponds to ~ 25 perfectly tagged $J/\Psi K_s^0$ events.

We use a negative log–likelihood method to determine the best value for $\sin 2\beta$. The B^0 lifetime and the Δm_d values are fixed to the world average values (1.54 ± 0.04 psec and 0.464 ± 0.018 psec^{-1}). The fit yields a value $\sin 2\beta = 0.79^{+0.41}_{-0.44}$ (stat. + syst.) for all the taggers combined [8]. In Figure 2 we show the distributions of the asymmetry both for the SVX and for the non–SVX samples. The precision of our direct measurement of $\sin 2\beta$ is still dominated by the statistical uncertainty (±0.36). This measurement provides for the first time an indication of CP violation in the B system, and it is consistent with the SM expectations.

Definite observation of CP violation in the B mesons requires a better precision. In Run II, with an integrated luminosity of ~ 2 fb^{-1}, we expect to reconstruct $\sim 10^4 J/\Psi K_s^0$ from dimuons, which will give a total uncertainty of about ±0.08. Triggering on $J/\Psi \to e^+e^-$ may increase the sample by 50%. CDF is also upgrading the detector with a Time–of–Flight system which will help flavor identification.

3 Top Quark Cross Section

At the Tevatron top quarks are produced mainly in pairs, via $q\bar{q}$ annihilation, with a theoretically expected cross section of only about 5 pb [9]. After several years of data taking during Run I, only about 600 $t\bar{t}$ events were produced. When we fold in the geometrical acceptances, identification criteria and selection requirements, the data set becomes much smaller.

In the framework of the SM each top quark decays into a W and a b quark. The final state of a $t\bar{t}$ decay therefore has two W bosons and two b quarks. Direct evidence of the existence of the top quark was presented by CDF [10] in early 1994. Later, in 1995, both the CDF and the DØ collaborations announced conclusive discovery of the top quark [11]. A key to the identification of $t\bar{t}$ events has proved to be the ability to *tag* the b quarks. Tagging of b quarks can be achieved at CDF using the silicon micro-vertex detector (SVX), and we can attain a b tagging efficiency of about $\sim 50\%$ in a $t\bar{t}$ event, by finding a secondary vertex from the interaction point (SVX tagging). Also, we can identify b quarks by means of a lepton (e or μ) from b decays, with an efficiency of $\sim 20\%$. This method is referred to as Soft Lepton Tagger (SLT). We measure the $t\bar{t}$ production cross section in several decay channels and all the channels yield consistent results. A final result is obtained by combining the cross sections in the individual channels.

In this paper we report on an improved measurement of the $t\bar{t}$ cross section in the "lepton+jets" channel, where one W decays leptonically and the other W decays hadronically. Here, we identify the b quarks through the SVX tagging method. This yields our most precise determination of the $t\bar{t}$ cross section in a single channel. In the data selection we require the presence of one lepton (e or μ), a large value of $\not{E}_T$ ($\not{E}_T > 20$ GeV), and at least 3 jets with $E_T > 15$ GeV and $|\eta| < 2.0$ [12]. The dominant backgrounds come from W+jets production and QCD multi–jet processes. The selection criteria are identical to what is described in Ref. [11], with a few exceptions.

Here, we outline the improvement used in this measurement and the differences with the previous result. The main difference in our measurement consists of a revised determination of the efficiency of the SVX tagging algorithm. We measure the tagging efficiency in the data and in simulated events.

The previous result used a method which determined the b–tagging efficiency using a Monte Carlo (MC) simulation, tuned to give the same track finding efficiency as in the data. The new method directly compares the b–tagging efficiencies in low–P_T inclusive electron samples (rich in heavy flavor) from data and from simulation. We find that there is no E_T dependence of the data–to–MC b–tagging efficiency ratio, alleviating previous concerns about extrapolating the results from low E_T jets in the inclusive electron samples to jets in top events.

Also, the Run I SVX b–tagging efficiency for a $t\bar{t}$ event has increased from $\approx 43\%$ to $\approx 50\%$. Most of the difference is due to outdated b–lifetimes previously used in the MC, outdated B and D branching ratios, and slight inconsistencies in the modeling of the SVX geometry. Among other improvements, we use a slightly different event selection where we measure jet energies and $\not{E}_T$ with the z–vertex of the primary lepton, instead of the center of the detector. Also, we have a better selection of candidates from Z° bosons. The new selection finds about 20% more real Z°'s and rejects about 20% less fake Z°'s. We use a new method to calculate mistags that uses a parameterization of the negative tagging rate from all jet data after corrections for heavy flavor contribution to the negative tags. The associated uncertainty is 10% (instead of 40%). The rate of $W+\geq 1$ jets events is shown in Figure 3. We compute the $t\bar{t}$ production cross section from the excess of events with at least one b–tag in the $W+\geq 3$ jets sample. The whole excess is attributed to $t\bar{t}$ events. In 105.1±4.0 pb^{-1} of data we find 29 $W+\geq 3$ jet events with an expected background contribution of 8.0±1.0 events. The resulting new value of the top cross section in the lepton+jets channel using the SVX tagging algorithm is 5.1±1.5 pb.

We use the new value for the b–tagging efficiency, and apply the needed modifications to the calculation of the cross section values in the other decay channels. Then, we combine the results from the "lepton+jets" channel (including SLT) with the updated results from the dilepton and from the all–hadronic channels. We use a likelihood procedure, where we take into account the correlations between the backgrounds. The new result yields a combined $t\bar{t}$ production cross section of $\sigma_{t\bar{t}} = 6.5^{+1.7}_{-1.4}$ pb, which can be compared to our previous value of $7.6^{+1.8}_{-1.5}$ pb.

4 Higgs Searches

4.1 SM Higgs

The SM provides a simple mechanism for spontaneous symmetry breaking through the introduction of a scalar field doublet. The doublet has one single observable scalar particle, the Higgs boson, with an unknown mass but with fixed couplings to other particles. At the Tevatron one is more likely to observe the WH and ZH production processes. In fact, although the Higgs production cross section from gluon–gluon fusion ($gg \rightarrow H$) is larger (by a factor of ~ 3 for a Higgs mass of 100 GeV/c^2 [13]) than the associated production of VH ($V = W^{\pm}, Z^{\circ}$), the decay products from $H \rightarrow b\bar{b}, \tau\bar{\tau}$ are difficult to disentangle from the di–jet QCD background. Instead, when the Higgs is produced in association with a V boson, we can use the presence of an additional lepton or additional jets (possibly from $W^{\pm}$ or Z°) to discriminate from background sources and use the b–tagging algorithm to identify b–jets from $H \rightarrow b\bar{b}$ events. The Tevatron is mostly sensitive in the region for $80 \leq M_{H_{SM}} \leq 130$ GeV/c^2 [14], where the branching ratio of $\mathcal{B}(H \rightarrow b\bar{b})$ is dominant.

We study various channels with different signatures in the final state. We search for the SM Higgs in the lepton+jets channel, in $q\bar{q} \rightarrow WH \rightarrow l\bar{\nu}b\bar{b}, ZH \rightarrow llb\bar{b}$ events. We look for an isolated high–p_T lepton $+\not{E}_T$ to identify W decays or pairs of leptons to identify Z° decays, and jets with b tags to identify the $H \rightarrow b\bar{b}$ decays. We also search for the Higgs in multi-jet events with ≥ 4 jets ($q\bar{q} \rightarrow W/ZH \rightarrow jjb\bar{b}$), of which at least two jets are b–tagged. Finally, we look for signatures with large $\not{E}_T$ from the process $q\bar{q} \rightarrow ZH \rightarrow \nu\bar{\nu}b\bar{b}$. In this analysis we start with a $\not{E}_T$ data sample (with $\not{E}_T > 35$ GeV) and require at least 2 b–tagged jets. We observe no deviations from the known SM backgrounds, in any of these final states. Therefore, we combine the results from the different channels and obtain an upper limit on Higgs production. Figure 4 shows the 95% C.L. upper limit results on $\sigma(VH^{\circ}) \cdot BR(H^{\circ} \rightarrow b\bar{b})$. The results indicate that the measurements at the Tevatron are not yet sensitive to the discovery of the SM Higgs, due to the small number of expected events.

We have studied the feasibility of SM Higgs search in Run II. We expect to improve our b–tagging capabilities, due to an increased acceptance [15] of our micro-vertex detector, by about 50% in events with single b tagging. Also in the future, the improvement of the di–jet mass resolution will be crucial for observing the Higgs boson. Therefore, we have studied a new algorithm for improving the jet energy resolution in the Run I data sample. We have measured an improvement of more than 25% as compared to our standard algorithm for single jet energy resolution, in a photon+jet sample (see Figure 5). In di–jet events we could expect an improvement on the di–jet mass resolution of an additional factor of $\sqrt{2}$. We combine results from the CDF and DØ experiments at the Tevatron as well as several channels. We include WH and ZH channels with the Higgs decaying into $b\bar{b}$ pairs for a Higgs mass below 130 GeV, while for a higher mass the $H \rightarrow WW$ decay has also been considered. Figure 6 shows the expectations once we include a better di–b jet mass resolution and the new detector acceptance. The integrated luminosity needed per experiment for a 5σ and 3σ discovery, and 95% C.L. limit is plotted as a function of the SM Higgs mass. Instead, if we use the present di–jet mass resolution, the luminosity needed to achieve the same results approximately doubles.

4.2 MSSM Higgs

The Minimal Supersymmetric Model (MSSM) [16] is a further extension of the SM. In the MSSM, a more complex symmetry breaking mechanism occurs. Five observable scalar particles are predicted: two charged ($H^{\pm}$) and three neutral (h°, H°, and A°) Higgs bosons. In the enlarged Higgs sector two new parameters are introduced: $\tan\beta$ which is the ratio of the vacuum expectation values of the two Higgs doublets, and the Higgs mass parameter μ.

At the Tevatron, h°, H° and A°, can be produced similarly to SM Higgs. In the MSSM, at large values of $\tan\beta$, the Higgs couplings to $\tau^+\tau^-$ and $b\overline{b}$ pairs are greatly enhanced. The coupling is approximately proportional to $(\tan\beta)^2 \sim (m_{top}/m_b) \sim 1000$. This results in a large production cross section in $p\overline{p} \rightarrow b\overline{b}h^{\circ}, b\overline{b}H^{\circ}, b\overline{b}A^{\circ}$ events (the same would happen for production in association with $\tau^+\tau^-$ pairs). At CDF we have searched for events with ≥ 4 jets (of which ≥ 2 b–tagged jets) in the final state. The number of events found in the data is in good agreement with the expected backgrounds (mainly from QCD events, from mistags, and from $Z^{\circ}jj$). We can set a 95% C.L. limit on the mass of MSSM neutral Higgs as a function of $\tan\beta$. These results are preliminary and not presented at the time of this conference.

In the charged Higgs sector instead, we have sensitivity at low values of $\tan\beta$ where $H^+ \rightarrow c\bar{s}$, and at large values of $\tan\beta$ where $H^+ \rightarrow \tau\nu$. We presented results on direct and indirect Higgs production from top quark decays $t \rightarrow H^+ b$, in both regions of $\tan\beta$. We do not find any anomalous excess of events over the expected background and set a limit on Higgs production. Results have not changed since [17]. At large values of $\tan\beta$, we can also use the results from a search for top quark pair production in the $e\tau + \not{E}_T$+jets and $\mu\tau + \not{E}_T$+jets signatures [18]. Here, we exploit the competing decays $t \rightarrow H^+ b$ and $t \rightarrow W^+ b$, when $W^+, H^+ \rightarrow \tau^+\nu$. In the region at large values of $\tan\beta$ the tbH^+ Yukawa coupling may become non–perturbative (see Ref. [19]). Therefore we choose to use a parameter–independent space to determine the excluded region. We can set a 95% C.L. upper limit on the branching ratio of $\mathcal{B}(t \rightarrow H^+ b)$ in the range 0.5 to 0.6 at 95% C.L. for Higgs masses in the range 60 to 160 GeV [20], assuming the branching ratio for $H^+ \rightarrow \tau\nu$ is 100% . The τ lepton is detected through its 1–prong and 3–prong hadronic decays.

5 SUSY Searches: stop and sbottom quarks

The range and complexity of SUSY signatures is growing fast. In the analysis of Run I data it has become evident that the use of heavy flavor tagging is gaining importance and it has become crucial. Here, we present the results from a recent analysis which searches for scalar quarks in events with $\not{E}_T$+jets. The signature comes from the decays of the supersymmetric particles decaying to jets and to neutralinos. We look for scalar top ($\tilde{t}_1$) and for scalar bottom ($\tilde{b}_1$) quarks in events with similar final states [21].

We search for the scalar top quark in events with large $\not{E}_T$ and with a pair of heavy flavor jets, from the decay $p\overline{p} \rightarrow \tilde{t}_1\overline{\tilde{t}_1} \rightarrow (c\tilde{\chi}_1^{\circ})(\bar{c}\tilde{\chi}_1^{\circ})$. We assume that the neutralino $\tilde{\chi}_1^{\circ}$ is the lightest supersymmetric particle and it is stable. From a data sample of 88 pb^{-1}, we select events with two or three jets, no leptons, and with $\not{E}_T > 40$ GeV. The requirement of large $\not{E}_T$ eliminates almost completely the QCD di–jet background. We require that $\not{E}_T$ is neither parallel nor anti-parallel to any jet direction in order to suppress contributions from QCD events where missing energy comes from jet energy mismeasurement. We use a “Jet Probability” (JP) algorithm to tag jets with a heavy flavor content. The JP algorithm relies on determining a probability that a jet originates from a secondary vertex, and it is optimized for charm or bottom selection in stop or sbottom searches. The probability that the tracks in a jet come from the primary vertex is flat and distributed between 0 and 1 for tracks originating from the primary vertex, and peaks at zero for tracks from a secondary vertex. The efficiency of the JP algorithm to tag charm quarks is checked in a charm enriched sample, with D^* and D° mesons. In our final data sample we find 11 events consistent with an expected background of 14.5±4.2 events from SM sources. We interpret the null result in the scalar top search as an excluded region in $m_{\tilde{t}_1}$ versus $m_{\tilde{\chi}_1^{\circ}}$ parameter space using a background subtraction method [22]. The 95% C.L. limit excluded region is shown in Figure 7.

Also, as we mentioned earlier, we can use similar selection criteria and search for scalar bottom quarks in the decay channel $p\overline{p} \rightarrow \tilde{b}_1\overline{\tilde{b}_1} \rightarrow (b\tilde{\chi}_1^{\circ})(\bar{b}\tilde{\chi}_1^{\circ})$. After we apply our final selection cuts, we find 5 events in the data sample, with an expected background from SM sources of 5.8±1.8 events. Figure 8 shows the 95% C.L. limit in the $m_{\tilde{b}_1}$ versus $m_{\tilde{\chi}_1^0}$ plane.

6 Conclusions and Prospects

We have presented some of the latest results obtained at CDF during Run I. Still, four years after the end of Run I, many analyses are being completed and many are still in progress. In Run II, both the CDF and the DØ detectors will be much more powerful, with much improved vertex detectors and tracking system which allow for larger acceptance and for higher efficiency in flavor tagging. The new upgraded detectors will collect more data at a higher energy of $\sqrt{s} = 2$ TeV. At this energy, the production cross section of heavy particles in the SUSY zoo for example, will increase significantly. Furthermore, with a factor of 20 in expected delivered luminosity during Run II, the experiments at the Tevatron will have a great chance to shed light into the new world of "new physics". Most importantly, by extending Run II up to an integrated luminosity of about 20 fb^{-1} and combining search channels, the Tevatron can perform a crucial test of the MSSM Higgs boson sector. The W and top quark mass measurements, from the Tevatron (both from CDF and from DØ) and from the LEP2 experiments, suggest a small value for the Higgs boson mass (see Figure 9). Also, most theories predict a Higgs mass which is comprised between 130 and 150 GeV/c^2. When combining these informations together, the picture looks promising for the Higgs searches at the Tevatron during Run II. The experience gained from Run I analyses will greatly increase the quality of the Run II searches. New triggering capabilities will open previously inaccessible channels. In conclusion, the upcoming Run II at the Tevatron appears as an exciting field of promises.

7 Acknowledgments

I would like to thank the organizers of this conference for a wonderful workshop and a marvelous hospitality. In particular I appreciated the discussions and direct contact with many of the participants at the conference to understand and update my knowledge of the results from the current experiments, in the sparse field of high–energy physics. Most of all, I would like to thank my collaborators for providing me with all of these results. In particular, I would like to thank Gerry Bauer for meticulously revising the manuscript and for his many suggestions in the difficult path of life. I would also like to thank Luc Demortier for his comments on the text and Stefano Lami for his constant wisdom.

References

[1] F. Abe *et al.* (CDF Collaboration), Nucl. Instrum. Methods A **271**, 387 (1988)

[2] N. Cabibbo, Phys. Rev. Lett. **10**, 531 (1963); M. Kobayashi and T. Maskawa, Prog. Theor. Phys. **49**, 652 (1973)

[3] J. Bartelt *et al.* (CLEO Collaboration), Phys Rev. Lett. **71**, 1680 (1993); F. Abe *et al.* (CDF Collab.) Phys. Rev. D **55**, 2546 (1997); K. Ackerstaff *et al.* (OPAL Collab.) Z. Phys. C **76**, 401 (1997)

[4] In the present analysis we extend the SST algorithm to the non–SVX sample, as it is explained later in the text. In the following literature you will find the description of the SST algorithm for the events comprised within the SVX acceptance: F. Abe *et al.* (CDF Collaboration), *Phys. Rev. Lett.* **81**, 5513 (1998); F. Abe *et al.* (CDF Collaboration), *Phys. Rev.* D **59**, 032001 (()1999); K. Kelley, Ph.D. dissertation, Massachusetts Institute of Technology (1999) (unpublished)

[5] F. Abe *et al.* (CDF Collaboration), *Phys. Rev. Lett.* **80**, 2057 (1998); P. Maksimović, Ph.D. dissertation, Massachusetts Institute of Technology (1998) (unpublished).

[6] The SLT algorithm used in this analysis is similar to the one used in: T. Abe *et al.* (CDF Collaboration), FERMILAB–PUB–99/019–E, to be published in *Phys. Rev.* D; M. Peters, Ph.D. dissertation, U. of California, Berkeley (1998) (unpublished).

[7] The JETQ algorithm used in this analysis is similar to the one used in: T. Abe *et al.* (CDF Collaboration), FERMILAB–PUB–99/019–E, to be published in *Phys. Rev.* D; O. Long, Ph.D. dissertation, U. of Pennsylvania (1998) (unpublished).

[8] T. Affolder *et al.* (CDF Collaboration), FERMILAB–PUB–99/225–E, submitted to *Phys. Rev.* D.

[9] E. Laenen *et al.*, *Phys. Lett.* B **321**, 254 (1994); E. L. Berger, H. Contopanagos, *Phys. Lett.* B **361**, 115 (1995); S. Catani *et al.*, *Phys. Lett.* B **378**, 329 (1996); R. Bonciani *et al.*, *Nucl. Phys.* B **529**, 424 (1998).

[10] F. Abe *et al.* (CDF Collaboration), *Phys. Rev.* D **50**, 2966 (1994).

[11] F. Abe *et al.* (CDF Collaboration), *Phys. Rev. Lett.* **74**, 2626 (1995); S. Abachi *et al.* (DØ Collaboration), *Phys. Rev. Lett.* **74**, 2632 (1995).

[12] In the CDF coordinate system, θ and ϕ are the polar and azimuthal angles, respectively, with respect to the proton beam direction. The pseudorapidity η is defined as $-\ln\tan(\theta/2)$. The transverse momentum of a particle is $P_T = P\sin\theta$. The analogous quantity using energies, defined as $E_T = E\sin\theta$, is called transverse energy. The missing transverse energy $\not\!\!E_T$ is defined as $-\sum E_T^i\,\hat{r}_i$, where $\hat{r}_i$ are the unit vectors in the transverse plane pointing to the energy depositions in the calorimeter.

[13] A. Stange, W. Marciano, and S. Willenbrook, *Phys. Rev.* D **49**, 2 (1994).

[14] J.F. Gunion, A. Stange and S. Willenbrock hep–ph/9602238.

[15] J. Conway, Proc. of 13th Les Rencontres de Physique de la Valle D'Aoste: Results and Perspectives in Particle Physics, La Thuile, Valle d'Aoste, Italy, February 28 – March 6, 1999; FERMILAB-CONF–99/156–E.

[16] For an introduction, see Martin, S.P., *A Supersymmetry Primer*, in *Perspectives on Supersymmetry*, G. Kane ed., World Scientific, 1998.

[17] M. Gallinaro, Pub. Proceedings 5th International Workshop on Tau Lepton Physics (TAU 98), Santander, Spain, September 14–17, 1998, FERMILAB–CONF–98/381–E.

[18] F. Abe *et al.* (CDF Collaboration), Phys. Rev. Lett. **79**, 3585 (1997).

[19] J.A. Coarasa, J. Guasch, J. Sola, Preprint UAB–FT–451, Feb. 1999, hep–ph/9903212.

[20] T. Affolder *et al.* (CDF Collaboration), Paper in preparation, to be submitted to *Phys. Rev.* D.

[21] T. Affolder *et al.* (CDF Collaboration), FERMILAB–PUB–99–311–E; submitted to *Phys. Rev. Lett.*; C. Holck, Ph.D. dissertation, U. of Pennsylvania (1999) (unpublished).

[22] C. Caso *et al.*, Eur. Phys. J. **C3**, 1 (1998).

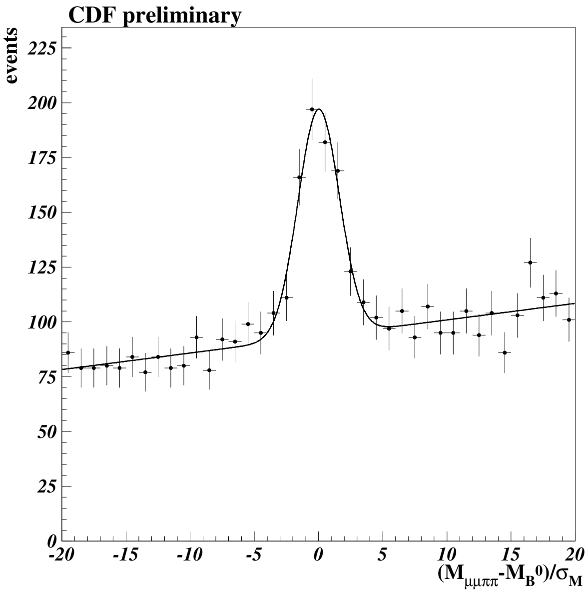

Figure 1: Mass distribution of the $J/\Psi K_s^0$ candidates. The fit of a gaussian distribution plus a linear background fit agrees well with the data. The invariant mass distribution is normalized to the world average B_d° mass (M_{B°), and to the uncertainty in the fit ($\sigma_M \sim 10$ MeV/c^2).

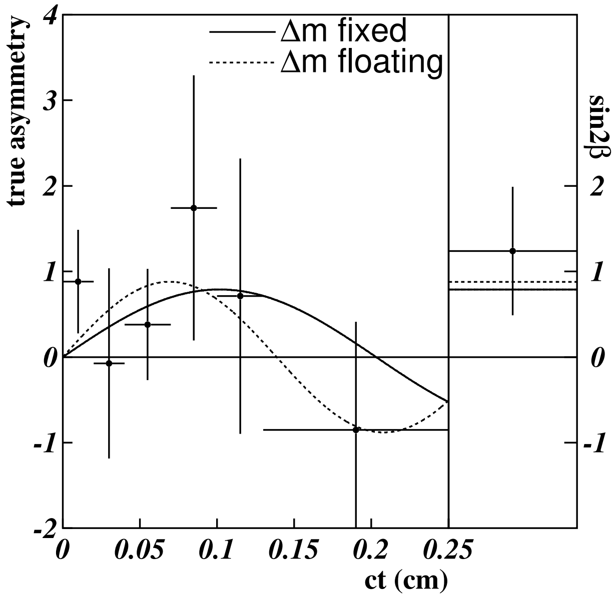

Figure 2: The true asymmetry as a function of lifetime for $B \to J/\Psi K_s^0$ events. The SVX data is shown in proper time bins on the left, and a single bin for non–SVX data on the right.

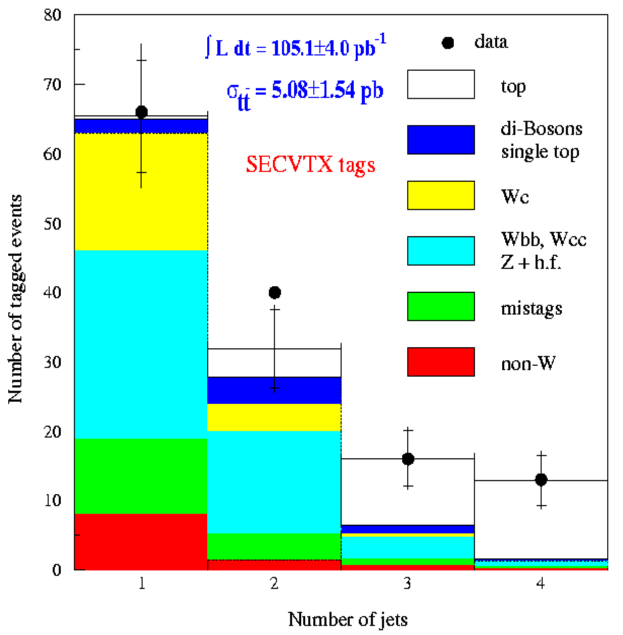

Figure 3: Observed and expected number of events with SVX tags. The vertical bars represent the overall uncertainty on the expected number of tags, and the horizontal ticks on the bars mark the contribution from the statistical uncertainty.

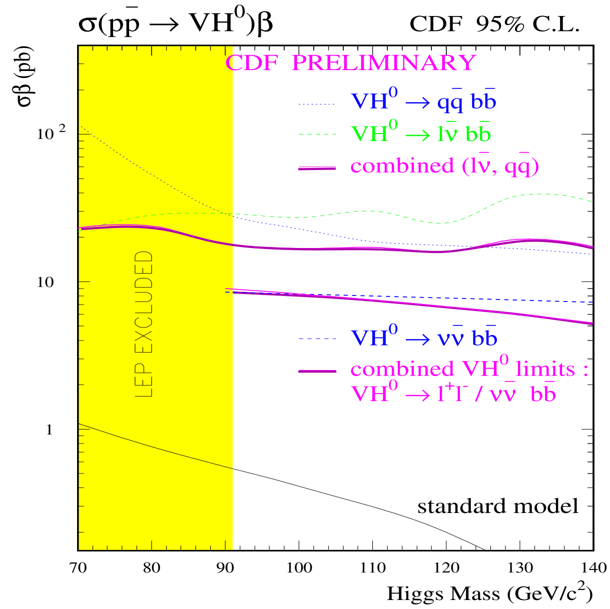

Figure 4: Upper limit on $\sigma(VH^\circ)\cdot BR(H^\circ \rightarrow b\bar{b})$, where $V = W, Z$, from individual and combined $VH^\circ \rightarrow l\nu b\bar{b}, q\bar{q}b\bar{b}, l^+l^-b\bar{b}, \nu\bar{\nu}b\bar{b}$ channels.

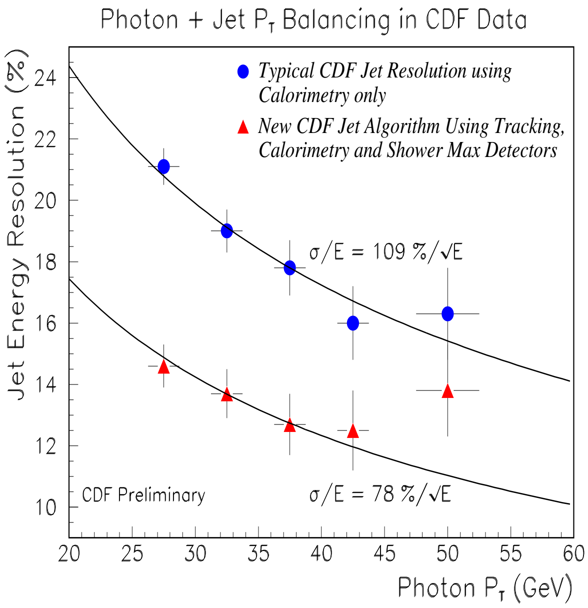

Figure 5: The jet energy resolution plotted as a function of photon p_T. We compare the results from a new improved algorithm to our standard method.

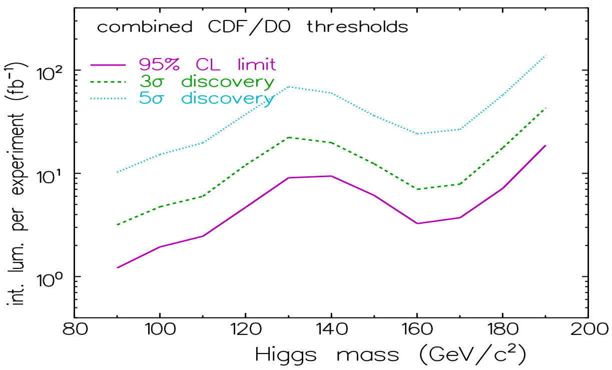

Figure 6: The integrated luminosity per experiment needed for a 5σ and a 3σ discovery, and 95% C.L. limit is plotted as a function of the Higgs mass. CDF and DØ results are combined as well as several channels. We include in the simulation an improvement of 30% in the di–jet mass resolution over Run I, and the new Run II detector acceptance.

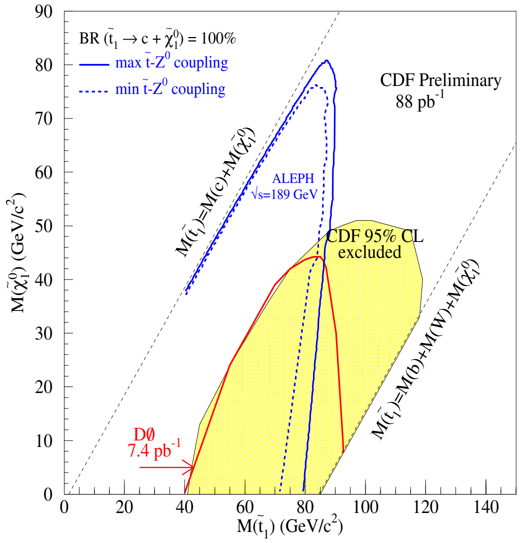

Figure 7: The 95% C.L. exclusion region (shaded region) in the plane $m_{\tilde{\chi}_1^\circ}$ versus $m_{\tilde{t}_1}$ for $\tilde{t}_1 \rightarrow c\chi_1^\circ$. Also shown are results from DØ and OPAL.

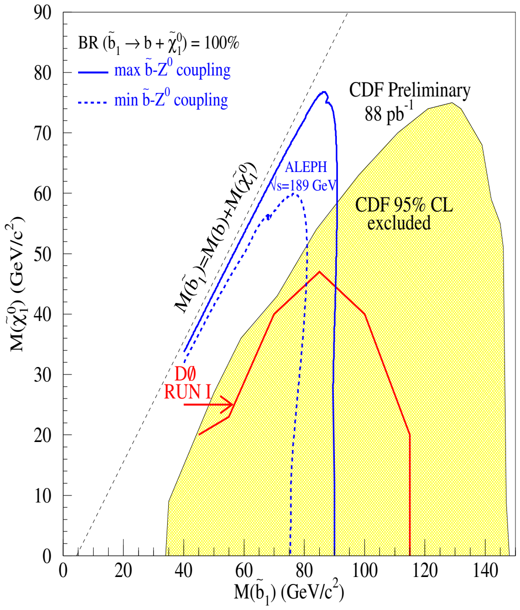

Figure 8: The 95% C.L. exclusion region (shaded region) in the plane $m_{\tilde{\chi}_1^\circ}$ versus $m_{\tilde{b}_1}$ for $\tilde{b}_1 \rightarrow b\chi_1^\circ$. Also shown are results from DØ and OPAL.

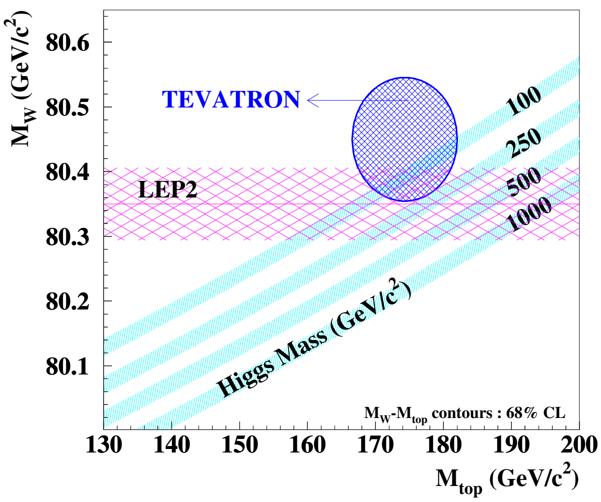

Figure 9: The measurements of the top quark and W boson masses performed at the Tevatron (from both CDF and DØ) and at LEP2 superimpose on different predictions for the value of the Higgs mass.